Organic carbon mineralisation in Iberian Margin sediments

Wim Helder and Eric Epping

Netherlands Institute for Sea Research - Dept. Marine Chemistry and Geology
P.O. Box 59, 1790 AB, Texel, The Netherlands

INTRODUCTION

Despite the fact that ocean margin sediments comprise only 16% of the global ocean area, they account for about 85% of the material accumulating in the ocean and 80-90% of the mineralisation in marine sediments. Shelf morphology and local hydrodynamical conditions may significantly influence the partitioning of material entering the ocean (land run-off or *in situ* production) between shelf sediments and the deeper ocean margin sediments. In this respect the Iberian Margin represents a narrow shelf interspersed with canyons, adjacent to north Atlantic abyssal plains. The rather complex circulation is dominated by a wind driven surface current in southward direction during summer and a density driven poleward current during the winter. The equatorward slope/shelf current during summer is generally associated with a band of cold upwelled North Atlantic Deep Water, which supports a high primary production along the Iberian Margin. During spring and summer, filaments of upwelled cold water move offshore and may allow the exchange of water and suspended matter between the coastal area and open ocean. The presence of upwelling filaments and canyons with their associated hydrography may represent additional means of transport for suspended matter, including organic carbon, to the deep-sea.

We participated in two cruises to construct budgets for organic carbon in sediments along different transects at the Iberian Margin. The first cruise (*PE121*, 30th July-17th August 1998) focussed on the 'normal' shelf-slope-abyssal settings for the Iberian Margin, whereas the second cruise (*PE138*, 8th May-1st June 1999) also included a transect in the Nazaré Canyon to assess the contribution of canyons to of-shelf-transport. In this annual report we present our results for the *PE121* cruise in 1998 and, when appropriate, will put this into perspective with previous findings for the Goban Spur area and the latest results from the *PE138* cruise in 1999.

MATERIALS AND METHODS

Once deposited at the seafloor, organic carbon can either be mineralized or buried in the sediment, depending on the degradability of the carbon. Thus, by estimating the rates of carbon mineralisation and carbon burial, the input of organic carbon (*i.e.*, the carbon deposition flux) to the sediment can be calculated by summing these quantities.

The rate of organic carbon mineralisation can be estimated from the rate of oxidant utilization (oxygen, nitrate, Mn_{ox}, Fe_{ox}, sulphate) and/or from the production rate of metabolites (ammonium, phosphate, dissolved inorganic carbon). These rates can be calculated from pore water profiles by predicting the downward flux of oxidants or the upward flux of metabolites, assuming one-dimensional Fickian diffusion:

$$flux = -\frac{D_0}{F} \times \frac{dC}{dz} ,$$

where D_0 is the temperature and salinity corrected free solution molecular diffusion coefficient, F is the sediment resistivity factor, and $\frac{dC}{dz}$ is the concentration gradient of the solute of interest. In addition fluxes can be measured directly by monitoring the concentration of solutes in a volume of water overlying a known area of sediment.

The carbon burial rate, F_b, can be estimated from

$$F_b = (1-f) \times r_s \times C_{org} \times w$$

where ω denotes the sediment accumulation rate, ϕ is the sediment porosity, ρ_s is the bulk sediment density, and C_{org} is the weight percentage of organic carbon. Sediment mixing rates as determined by ^{210}Pb profiles and sediment accumulation rates were provided by de Stigter and van Weering (Partner 5a).

IN SITU MEASUREMENTS

Oxygen profiles and *in situ* nutrient fluxes

The role of oxygen in organic carbon mineralisation changes from the regeneration of oxidants in areas of high organic carbon input, to being the dominant terminal electron acceptor in areas of low organic rain rates. Therefore, the oxygen consumption rate of the sediment, expressed as the sediment-water flux of oxygen, is a good indication for the carbon mineralisation rate. These fluxes can be assessed directly by monitoring the change in oxygen concentration in the water overlying an enclosed area of sediment, or can be calculated from the oxygen concentration gradient across the sediment-water interface. The concentration profiles of oxygen enable the estimation of oxygen consumption as a function of depth in the sediment, which can be used as an index for the degradability of the organic matter (Figure 1, left panel). However, these measurements represent point measurements and have virtually no areal integration. To encompass the lateral variability in reactivity and diffusive transport, benthic chambers were deployed for the direct measurement of oxygen fluxes.

The TROL (Temperature Resistivity and Oxygen Lander), a free falling vehicle was equipped with three incubation chambers and a profiling module. The profiling module was recently modified to allow the use of custom built Clark type oxygen microelectrodes. These electrodes had tip diameters of 10-20 µm, a stirring sensitivity < 1 %, an output of *ca.* 200 pA in air saturated seawater at 20°C, and were furnished with a guard electrode to ensure stable output currents. A resistivity sensor, modified after Andrews and Bennett, was used to determine the sediment-water interface and sediment resistivity. The benthic chambers, enclosing an area of 144 cm^2 were equipped with custom-built Clark type oxygen sensors with a guard electrode for continuously monitoring the oxygen concentration in the enclosed water column. These electrodes proved to give a very stable, low-noise signal, which allowed the calculation of oxygen uptake rates of the sediment (Figure 1, right panel). Additionally, 5 pairs of syringes allowed the manipulation of the overlying water during the time course of incubation. Two chambers were configured to determine the *in situ* fluxes of nutrients (ammonium, nitrate, nitrite, phosphate and silicate), and of dissolved inorganic carbon across the sediment-water interface. The third module was configured to inject sodium bromide, a conservative tracer in the enclosed overlying water. After incubation *in situ*, the enclosed sediment was retrieved and sliced to collect the pore water for bromide analysis (NIOZ lab). From these bromide pore water profiles, effective diffusion coefficients were estimated.

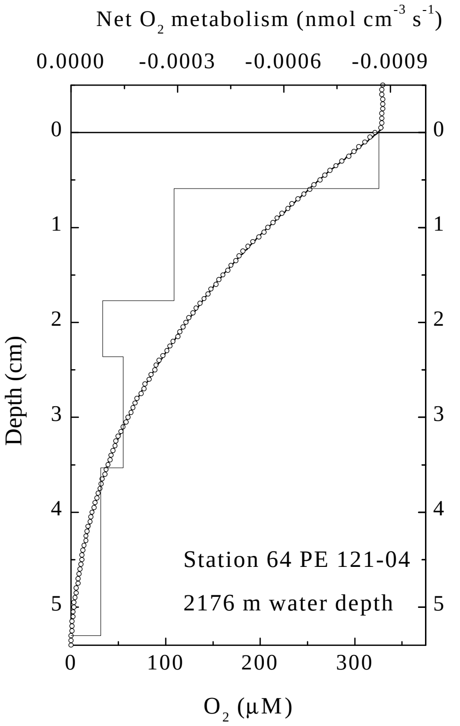

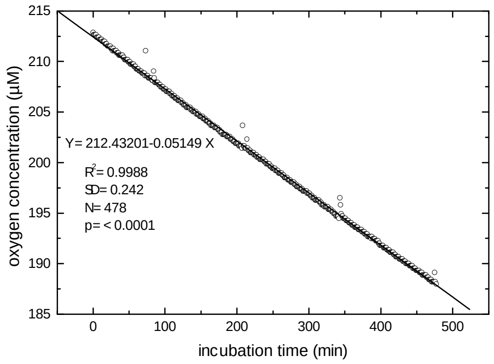

Figure 1. An example of an in situ oxygen profile recorded with the TROL (left) and a chamber incubation at 113-m water depth (above). The experimental profile in the left panel (circles) was fitted to estimate the rate of oxygen consumption as a function of depth (solid line)

SHIPBOARD PROCEDURES

Pore water and solid phase sampling

Sediment cores were obtained by multicoring. The corer retrieves four 10 cm (i.d.) cores and eight 6.5 cm (i. d.) cores. The sediment was extruded from the multi cores by a hydraulically operated core slicer, which facilitated the simultaneous processing of 4 multicores. Slices from identical depth intervals were pooled and homogenized. The pore water was separated from the sediment matrix by centrifugation at 3000 rpm for 10 minutes and subsequent filtration over 0.2 µm filters. Pore waters were analyzed for ammonium, nitrate, nitrite, phosphate, silicic acid, Fe_{dis}, Mn_{dis} and ΣCO_2 usually within 24 hours, using TRAACS 800+ autoanalysers. The solid phase was stored for organic carbon, total nitrogen, biogenic silica, and solid iron and manganese analysis in the laboratory.

Oxygen microprofiles

For the stations visited during the PE121 cruise, the concentration gradient of oxygen across the sediment-water interface was measured with a vertical resolution of 100 µm, using custom-built Clark type microelectrodes with internal guard. The oxygen profiles were measured in sediments, retrieved by multi-corer. The sediment surface was gently pushed up to the rim of the liner and the core was positioned in a flow chamber to create a ‘laminar flow’ over the sediment surface. The whole set up was incubated at *in situ* temperature. Two to six profiles were recorded for every station.

Sediment-water fluxes

Sediment-water fluxes were estimated by monitoring the concentration of solutes in the overlying water of 3 multicores (10 cm i.d.). In order to preserve the microtopography of the sediment-water interface, the overlying water of the cores was not replaced by filtered bottom water. The cores were incubated between 14 and 18 hours.

Geographical position of the sampling stations

Table 1 and 2 give an overview of the stations and activities during the *PE121* and *PE138* cruise, respectively.

Station	Water depth (m)	Position N	Position W	pore water extraction	Shipboard Oxygen profiling	Sediment-water Fluxes	TROL Deployed
Tansect 1							
1	4941	43.47	10.57	X	X	X	
2	3371	43.00	10.20	X	X	X	
3	2926	42.50	10.22	X	X	X	
4	2213	42.38	10.01	X	X	X	X
5	223	42.38	09.29	X	X	X	
Transect 2							
6	4908	44.00	10.00	X	X	X	
8	2109	43.43	09.24	X	X		
10	175	43.25	09.07	X	X	X	
Transect 3							
11	2073	42.00	09.44	X	X	X	
12	123	41.52	09.10	X	X	X	X
13	104	41.52	09.04	X	X		

Table 1. Overview of the geographical position, water depth, and activities for the stations visited during the PE121 cruise (30th July – 16th August 1998).

Station	Water depth (m)	Position N	Position W	pore water extraction	Sediment-water Fluxes	TROL Deployed
1	213	42.38	09.28	X	X	X
2	2164	42.38	10.00	X	X	X
3	2932	42.37	10.22	X	X	X
4	2060	42.00	09.44	X	X	X
5	2853	42.00	10.30	X	X	
6	113	41.52	09.04	X	X	X
7	1387	42.00	09.94	X	X	X
11	932	42.00	09.26	X	X	
12	344	39.39	09.15	X	X	X
13	137	39.39	09.20	X	X	
14	3097	39.31	09.51	X	X	X
15	396	39.35	09.37	X	X	
16	890	39.36	09.24	X	X	
17	4280	39.35	10.17	X	X	X

Table 2. Overview of the geographical position, water depth, and activities for the stations visited during the PE138 cruise (8th May – 1st June 1999).

RESULTS AND DISCUSSION

The organic carbon content of the uppermost sediment layers ranged from *ca.* 0.4% to 1.5%, the lowest values being associated with the shallow shelf stations, except for station 13 which shows a content of >2% (Fig. 2). The general trend shows the absence of a downcore gradient in organic carbon content at the shallow shelf stations, and an exponentially decaying content at greater water depth. At a water depth of *ca.* 2000 m, a rather strong surface gradient is observed which tends to decrease with increasing water depths. The atomic C/N ratios of organic carbon, considered to be indicative for the refractiveness of the organic carbon, range between 6 and 8 for all stations, except for the shelf stations 5 and 13 which show ratios between 10 and 15. This suggests that the bulk carbon at stations 5 and 13 consists of refractory carbon, presumably of terrestrial origin, whereas sedimentary organic carbon at the deeper stations originates from marine sources.

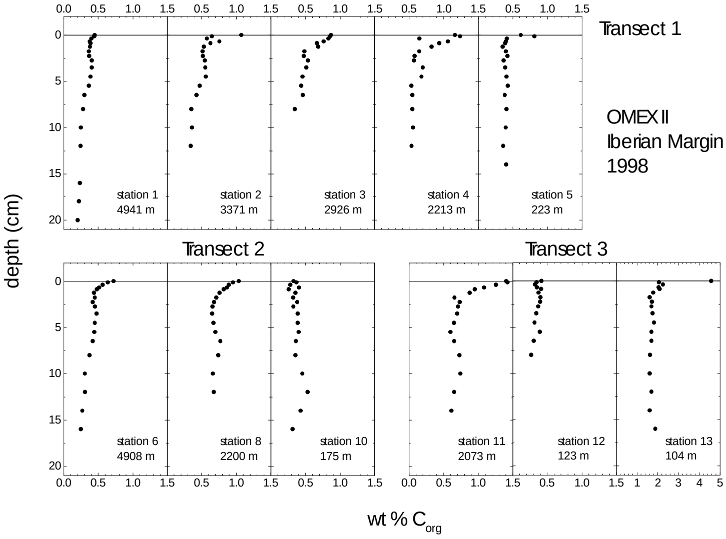

Figure 2. Sediment organic carbon profiles for the stations visited in 1998.

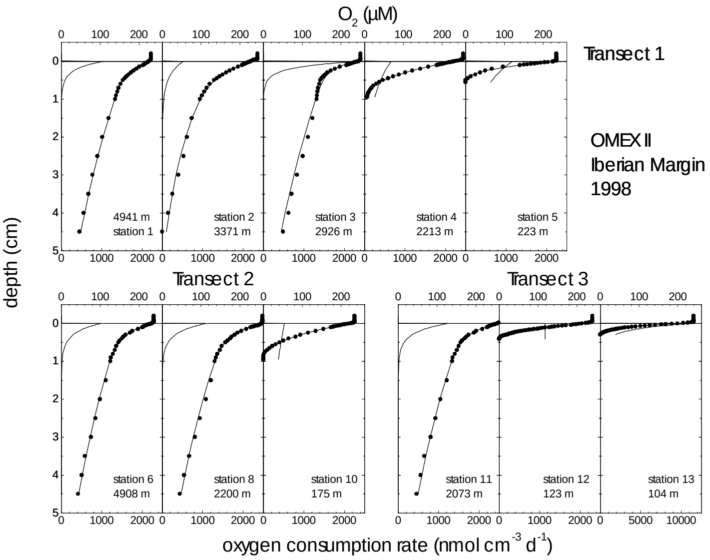

Figure 3. Experimental (symbols) and modeled (solid line) shipboard oxygen microprofiles, and calculated oxygen consumption activities.

Still, the shipboard oxygen microprofiles as displayed in Figure 3 indicate high rates of oxygen consumption at the shallow shelf stations, which decrease with increasing water depth. As a result, the oxygen penetration depth increased from *ca.* 0.4 cm at the shelf to >4 cm at depths exceeding 2000 m. The penetration depth at sediment trap station 4, though, is only 1 cm suggesting a rather high diagenetic activity as compared to station 8 and 11 at similar water depths.

The pore water profiles of nitrate (Figure 4), the second most important oxidant for organic carbon mineralisation, reveal that the maximum downward gradient and therefore the downward flux of nitrate decreases with increasing water depth. The nitrate profiles for station 4, 8, and11, representing the 2000 m stations for transect 1, 2, and 3, respectively, are rather similar and do not suggest enhanced diagenetic activity at the sediment trap station as did the shipboard oxygen profiles. A simple diffusion-reaction model (Goloway and Bender 1982, Bender and Heggie 1984) was used to predict carbon mineralisation rates from the nitrate profiles that show a distinct subsurface maximum in nitrate concentration. For the shelf stations that do not show this subsurface maximum, a simple first-order denitrification model was applied.

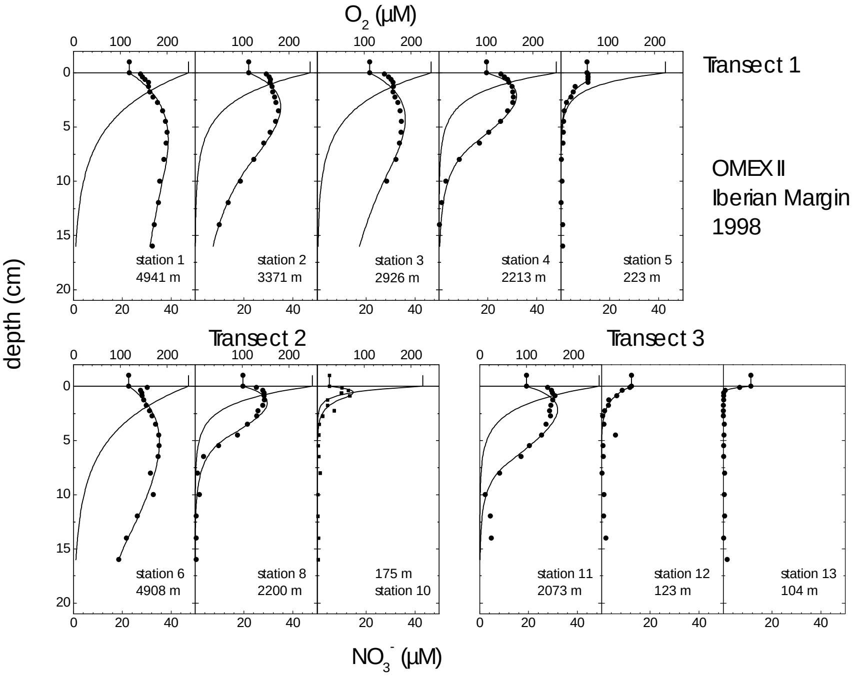

Figure 4. Nitrate pore water profiles (symbols) for the stations during the 1998 cruise. The curves reproducing the experimental data represent the best fit of the nitrate profile, whereas the second curve is the predicted oxygen profile, using the diffusion reaction model of Goloway and Bender 1982. For stations 12 and 13, a simple first-order diffusion-reaction model was applied without prediction of the oxygen profiles.

The predicted carbon oxidation rates using nitrate as oxidant ranged from 0.006 mmol C m^{-2} d^{-1} at 4941 m water depth to 0.089 mmol C m^{-2} d^{-1} at 175 m water depth. An extremely high value of 0.327 mmol C m^{-2} d^{-1} is observed for station 13 at 104 m water depth. At this station the overlying water appeared to be the main source of nitrate and the very thin oxic layer warrants a short transport time from the overlying water down to the anoxic sediment.

The model of Goloway and Bender (1982) also allows a prediction of the oxygen profile from the nitrate profile. Comparing these predicted profiles with the shipboard measured profiles reveals that the oxygen penetration depths estimated from the nitrate pore water profiles largely exceeds the penetration depths as actually measured. The oxygen fluxes and therefore the oxic carbon mineralisation rates as predicted from the nitrate profiles are much lower than estimated from the shipboard oxygen profiles. Such artifacts on shipboard oxygen profiles have been reported previously and have been attributed to decompression, warming of the core during the upcast of the multicorer *etc.* However, for the Goban Spur area no significant or systematic difference was observed between *in situ* profiles as recorded by TROL and shipboard oxygen profiles. In 1998, the TROL lander was modified to enable the use of guarded Clark type oxygen microelectrodes, which showed a superior performance as compared to the single-cathode-type oxygen electrodes. Electronic malfunctioning of TROL though, limited the number of successful deployments to 2 stations: the sediment trap station 4 at 2213 m and the sandy shelf station 12. A direct comparison between shipboard and *in situ* profiles on the one hand and between *in situ* single cathode and the new Clark type electrode on the other hand is presented for the sediment trap station 4 in Figure 5.

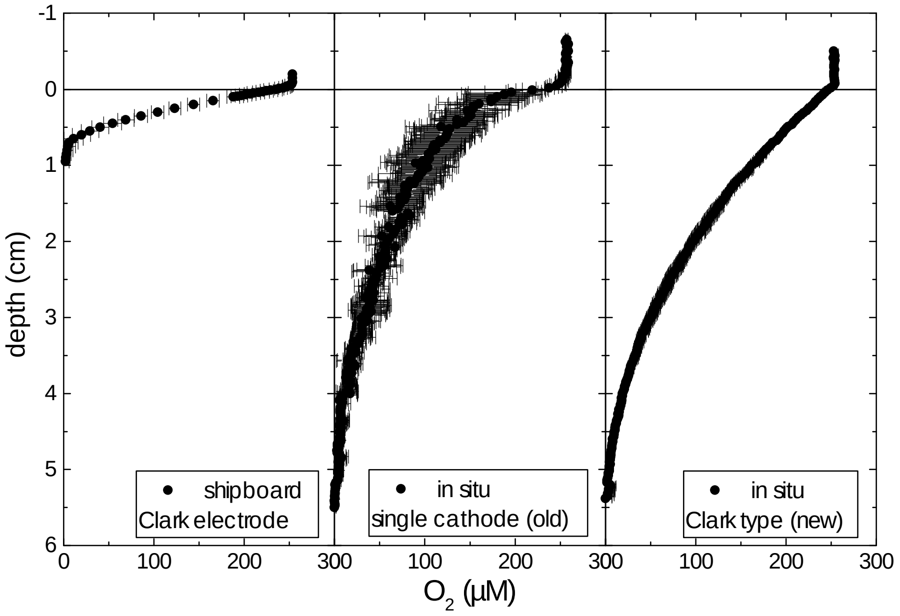

Figure 5. A comparison of shipboard and *in situ* measurement of oxygen (left and right panel) and of the single cathode type of oxygen microelectrode with the guarded Clark type electrode both applied *in situ*.

Despite the major difference in penetration depth between the shipboard and *in situ* profile with the single cathode electrode, the gradient across the interface and therefore the calculated fluxes of oxygen are very similar. The *in situ* profiles made by single cathode electrodes and the new Clark type electrodes show identical oxygen penetration depths, however, major differences were observed on the gradient across the surface. As a consequence, the new type of electrodes predict a lower oxygen flux. In addition, the Clark type electrodes suggest less spatial variability as compared with the single cathode type electrodes. From this comparison it is concluded that the modification as made on TROL represents a major improvement, which may allow the detection of seasonal variability in oxygen fluxes in future applications. A second implication is that oxygen fluxes at Goban Spur, though measured *in situ*, may have been overestimated due to this methodological artifact, especially at depths exceeding 2000 m.

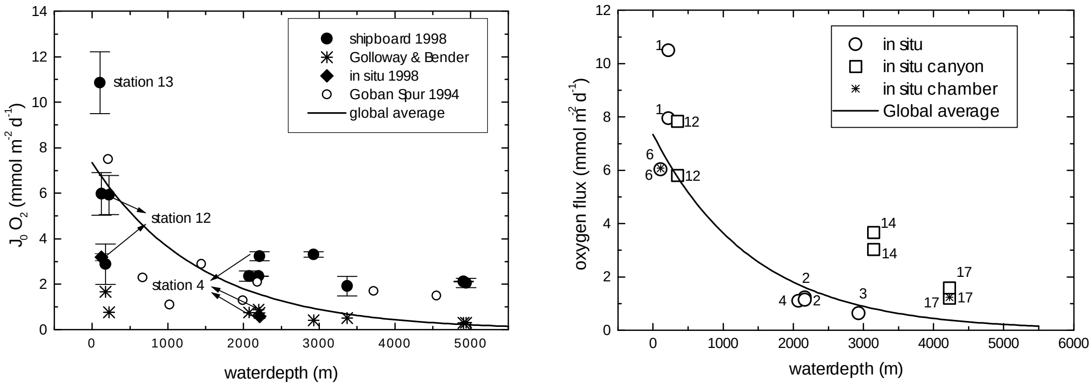

Figure 6. Oxygen fluxes as predicted from shipboard oxygen profiles, *in situ* profiles and from nitrate profiles (left panel) and oxygen fluxes as predicted from *in situ* profiles and chamber incubation in 1999 (right panel). The solid line represents the global trend for aerobic mineralisation as a function of water depth (Middelburg *et al.*, 1997)

This is confirmed by comparing the oxygen fluxes versus depth with the global average for aerobic mineralisation versus water depth as presented by Middelburg *et al.* (1997), which indicates that most of the experimental fluxes at depth >2000 m exceed the global average (Figure 6, left panel). The fluxes in 1999, all determined from data obtained by Clark type electrodes, correspond very well with the global average (Figure 6, right panel). In addition it shows that the oxygen fluxes in the Nazaré Canyon, as indicated by the open squares, are somewhat above the global average at the shelf (*ca.* 344 m), but exceed the global average by a factor of 4 and 3 at 3097m and 4280 m, respectively.

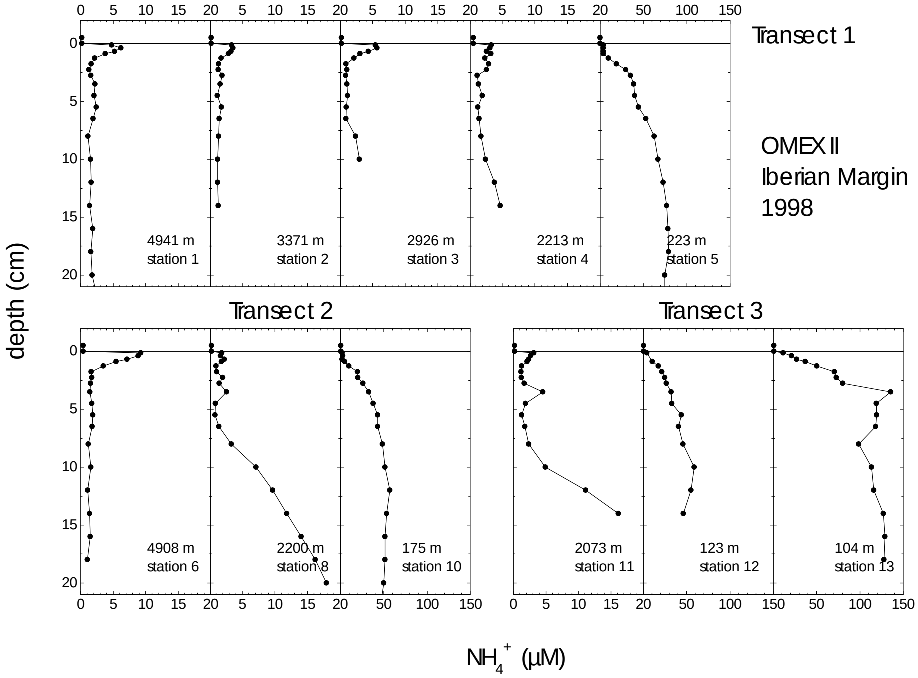

Figure 7. Ammonium profiles for the stations visited in 1998. From these profiles the rates of anoxic carbon mineralisation were estimated.

Anoxic mineralisation, as deduced from the ammonium pore water profiles in Figure 7, makes a significant contribution to organic carbon mineralisation only at the shallow shelf stations where it ranges from 0.4 mmol C m^{-2} d^{-1} at station 10 to 1 mmol C m^{-2} d^{-1} at station 13. At 2000-m water depth anoxic mineralisation accounts for 0.02 to 0.1 mmol C m^{-2} d^{-1}. At greater water depths, the contribution of anoxic carbon mineralisation becomes insignificant.

The carbon budgets as constructed from the burial and mineralisation rates for the stations visited during the PE121 cruise are presented in Table 3.

	burial flux	mineralisation	deposition	burial efficiency
station	mmol C m^{-2} d^{-1}			%
1	0.064	0.333	0.398	16.127
2	0.053	0.570	0.623	8.527
3	0.036	0.469	0.505	7.053
4	0.094	0.646	0.740	12.668
5	0.031	6.428	6.459	0.484
6	0.139	0.336	0.475	29.337
8	0.104	1.039	1.143	9.130
10	0.026	3.374	3.400	0.774
11	0.175	0.934	1.109	15.765
12	0.013	6.222	6.236	0.215
13	0.183	12.190	12.373	1.479

The deposition fluxes of organic carbon are dominated by the deposition of degradable carbon, since a major part is mineralized on time scales equivalent to *ca.* 20 cm sediment depth. This deposition flux of organic carbon decreases exponentially with water depth (Figure 8 left), whereas the burial efficiency reveals an increasing trend with water depth (Figure 8, right). Thus, the amount of carbon as well as the degradability of carbon arriving at the sea floor decreases with increasing water depth.

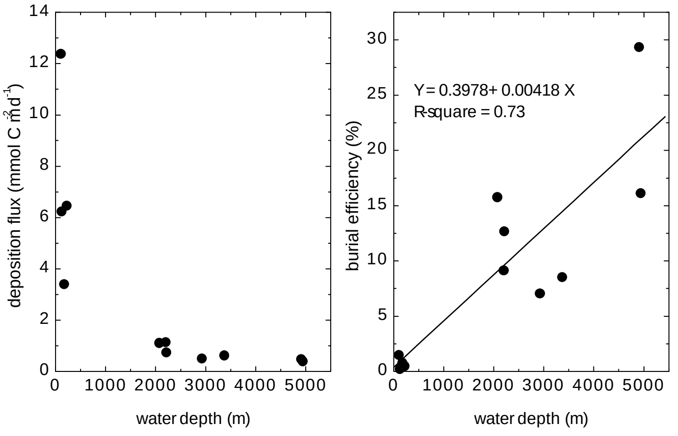

Figure 8. The deposition flux of organic carbon (left) and the burial efficiency of organic carbon (right) plotted *versus* water depth for the stations visited in 1998.

Whether these results are to be explained exclusively by the distribution of primary production and residence time in the water column before settlement, or whether lateral, of-shelf transport should be invoked remains to be evaluated by comparing these results with sediment-trap studies and primary production studies in this area.

The preliminary results presented above are obtained from simple, uncoupled diffusion-reaction models. Currently, the coupled diagenetic model OMEXDIA by Soetaert *et al.* (1996) is applied to obtain a better constraint on metabolic activities, sediment mixing rates and carbon qualities in sediments of the Iberian Margin.

REFERENCES

Bender, M.L. and Heggie, D.T. (1984). Fate of organic carbon reaching the deep sea floor: a status report. *Geochimica et Cosmochimica Acta*, 48: 977-986.

Goloway, F. and Bender, M. (1982). Diagenetic models of interstitial nitrate profiles in deep sea suboxic sediments. *Limnology and Oceanography*, 27: 624-638.

Middelburg, J.J., Soetaert, K. and Herman, P.M.J. (1997). Empirical relationships for use in global diagenetic models. *Deep-Sea Research* 44(2):327-344.

Soetaert, K., Herman, P.M.J. and Middelburg, J.J. (1996). A model of early diagenetic processes from the shelf to abyssal depths. *Geochimica et Cosmochimica Acta* 60:1019-1040.